Fibers and Polymers 2016, Vol.17, No.2, 220-228
DOI 10.1007/s12221-016-5838-8

ISSN 1229-9197 (print version)
ISSN 1875-0052 (electronic version)

Multifunctional Modification of Wool Fabric Using Graphene/TiO_2 Nanocomposite

Mohammad Ali Shirgholami, Loghman Karimi[1]*, and Mohammad Mirjalili

Department of Textile Engineering, Yazd Branch, Islamic Azad University, Yazd, Iran
[1]*Young Researchers and Elites Club, Science and Research Branch, Islamic Azad University, Tehran, Iran*
(Received November 13, 2015; Revised January 14, 2016; Accepted January 30, 2016)

Abstract: In this study, a new finishing technique is introduced through treatment of wool fabric with graphene/TiO_2 nanocomposite. Graphene oxide/titanium dioxide nanocomposite first applied on the wool fabric by hydrolysis of titanium isopropoxide in graphene oxide suspension and then this coating chemically converted by sodium hydrosulfite to graphene/TiO_2 nanocomposite. The homogenous distribution of the graphene/TiO_2 nanocomposite on the fiber surface was confirmed by field emission scanning electron microscopy (FE-SEM), Energy-dispersive X-ray spectroscopy (EDS) and X-ray mapping. X-ray diffraction patterns proved the presence of titanium dioxide nanoparticles with a crystal size of 127 Å on the treated wool fabric. Also, the defect analysis based on X-ray photoelectron spectroscopy (XPS) established the composition of the nanocomposite. Other characteristics of treated fabrics such as antibacterial activity, photo-catalytic self-cleaning, electrical resistivity, ultraviolet (UV) blocking activity and cytotoxicity were also assessed. The treated wool fabrics possess significant antibacterial activity and photo-catalytic self-cleaning property by degradation of methylene blue under sunlight irradiation. Moreover, this process has no negative effect on cytotoxicity of the treated fabric even reduces electrical resistivity and improves UV blocking activity.

Keywords: Multifunctional, Wool, Graphene/TiO_2 nanocomposite, Photocatalytic, Electrical conductivity

Introduction

Wool is one of the oldest fibers known to man and is widely used as a high quality textile material because of its unique natural properties (softness, warmth, lightness, etc.) [1]. As the consumers are constantly seeking improved performance and exciting new innovations, production of wool fabrics with multifunctional properties have became concerns of the textile industry. Nowadays, a demand for end-use textile field such as self-cleaning, antibacterial, electrical conductivity, UV blocking, and others can be achieved by application of nano-particles to textile materials. For instance, deposition of titanium dioxide nanoparticles on textiles provides new properties such as self-cleaning, UV-protection, superhydrophilic, antibacterial, flame retardancy, etc. [2-6]. Also, using silica nanoparticles for water repellency [7,8], zirconium dioxide for self-cleaning and flame retardancy [9,10], carbon nanotube for conductivity and water repellency [11,12], and silver for antimicrobial [13,14] was reported. Nano materials-loaded wool fabric could be used in medical and textile applications such as medical devices, healthcare, wound dressing, military, protective suits, personal care product, clothing and others [15].

The incessant progress of nanotechnology in material science has opened new pathways for developing new functional materials. Graphene, one-atom-thick planar sheets of sp^2-bonded carbon atoms that are densely packed into a 2-D honeycomb crystal lattice, has become one of the most attractive materials due its unique chemical and physical properties as well as its diverse potential applications [16, 17]. Some researchers produced electrically conductive fabrics by immobilizing graphene on the surfaces of fabrics [18-21]. Also, ultraviolet blocking and antimicrobial textiles obtained through applying the graphene [22,23].

In a mixture of graphene and titanium dioxide, graphene would act as an electron acceptor of the photo-generated electrons for TiO_2, contributing to the extension of recombination time for electron-hole pairs [24]. Also, the graphene's high surface area would improve the photocatalystic performance of titanium dioxide nanoparticles by expanding the photosensitivity under visible light [25]. The application of graphene/titanium dioxide nanocomposites for fabric finishing has also been recently reported and has shown its advantages [26-28]. Karimi *et al.* applied *in situ* synthesis of titanium dioxide on graphene oxide coated cotton fabrics using $TiCl_3$ as both reducing agent and TiO_2 precursor [26]. Also, they optimized photo-activity efficiency of the treated cotton fabrics using the response surface methodology [27]. Along the same lines, Molina and colleagues obtained photocatalytic fabrics based on reduced graphene oxide and titanium dioxide coatings on polyester fabrics [28].

Herein, the combination of titanium dioxide and graphene for imparting multi-functional properties, i.e. self-cleaning, electrical conductivity, ultraviolet (UV) blocking as well as antimicrobial properties onto wool fabric is studied. Graphene oxide/TiO_2-coated wool fabric was prepared by hydrolysis of titanium isopropoxide in graphene oxide suspension under ultrasound irradiation. Thereafter, the graphene oxide/TiO_2 coating chemically converted into graphene/TiO_2 by immersion of the coated fabrics in a sodium hydrosulfite solution.

*Corresponding author: l.karimi@srbiau.ac.ir

Experimental

Materials

The plain weave structure wool fabric was used with the fabric weight of 170 g/m^2. Graphite powder with particle size less than 20 μm was purchased from Sigma-Aldrich. Titanium isopropoxide ($C_{12}H_{28}O_4Ti$) as metal alkoxide reagent for producing nano titanium dioxide, sodium hydrosulfite ($Na_2S_2O_4$), sulfuric acid (H_2SO_4, 98 %), hydrogen peroxide (H_2O_2, 30 %), potassium permanganate ($KMnO_4$) and hydrochloric acid (HCl, 37 %) were prepared from Merck. Methylene blue (CI 52015) was provided by Uhao Co. (China).

Instrument

FE-SEM and X-ray mapping images and EDS patterns were established by MIRA3-TESCAN, field emission scanning electron microscope (FE-SEM) (Czech Republic). The X-ray diffraction (XRD) analysis was performed using a STOE (model STADI MP) X-ray Diffractometer, Germany. The patterns were recorded in the diffraction range of 2θ from angle of 10 ^{o} to 90 ^{o} with a scanning speed of 2 ^{o}/min at 2θ step of 0.040 ^{o}. Cu Kα radiation (λ=1.540 Å) with detector scan mode operating at 40 kV and 30 mA was used to investigate changes in crystalline. X-ray photoelectron spectroscopy (XPS) data were recorded using an X-ray 8025-BesTec XPS system (Germany) with an Al Ka X-ray source (hv=1,486.6 eV). Electrical surface resistivity of the fabrics was determined based on AATCC test method 76-2005 by means of the Hioki Digital HiTester Multimeter, model 3256-50, Japan. UV-blocking activities of the fabrics were recorded by using Perkin-Elmer Lambda 35 UV-vis spectrophotometer.

The electrochemical experiments were performed with an Autolab (Eco-Chemie, Ultrecht, and the Netherlands). All measurements were conducted at room temperature (25 ^{o}C) with a conventional three-electrode cell, which included a Ag/AgCl (saturated by 3 M KCl solution) as reference electrode, a platinum wire as counter electrode, and a wool coated fabric with graphene oxide/titanium dioxide nanocomposite or graphene/titanium dioxide nanocomposite as working electrode. Cyclic voltammograms (CVs) were carried out at a scan rate of 50 mVs^{-1} in a quiescent phosphate buffered saline (0.1 M, pH 7.0).

Methods

Synthesis of Graphene Oxide

Graphene oxide was synthesized by a modified Hummers method from natural graphite as previously reported [26]. The obtained graphene oxide was mixed with water, and then the dispersion was sonicated in an ultrasonic bath (WiseClean, 50-60 Hz) for 60 min. The final sonicated dispersion was centrifuged at 3000 rpm for 30 min and the non-exfoliated graphite oxide removed, resulting in a pure graphene oxide aqueous dispersion.

Synthesis of Graphene/TiO_2 Nanocomposite onto Wool Fabric

The wool fabrics were immersed into the aqueous suspension of graphene oxide with various concentrations. To synthesis graphene oxide/TiO_2 nanocomposite on the wool fabric,

Table 1. Experimental conditions and tests results

Graphene oxide concentration (w/v %)	Titanium isopropoxide (m*l*)	Electrical resistivity after reduction (Ω/square)	Electrical resistivity after washing (Ω/square)	E% Under sunlight
0.0	0	1×10^9	-[a]	3.3
	1	1.2×10^9	-[a]	16.4
	2	1.5×10^9	-[a]	26.2
	3	1.6×10^9	-[a]	32.4
	4	1.8×10^9	-[a]	38.3
	5	1.9×10^9	-[a]	39.8
0.02	0	495×10^6	-[a]	4.4
	1	500×10^6	-[a]	25.2
	2	500×10^6	-[a]	38.8
	3	500×10^6	-[a]	41.9
	4	505×10^6	-[a]	44.3
	5	505×10^6	-[a]	48.4
0.05	0	340×10^6	-[a]	6.5
	1	345×10^6	-[a]	30.4
	2	345×10^6	-[a]	43.1
	3	345×10^6	-[a]	45.5
	4	360×10^6	-[a]	49.9
	5	370×10^6	-[a]	53.5
0.1	0	300×10^6	-[a]	7.8
	1	310×10^6	-[a]	33.3
	2	315×10^6	-[a]	48.4
	3	315×10^6	-[a]	52.2
	4	320×10^6	-[a]	59.5
	5	320×10^6	-[a]	69.5
0.2	0	10×10^6	-[a]	10.2
	1	20×10^6	-[a]	45.3
	2	40×10^6	-[a]	58.8
	3	40×10^6	-[a]	69.6
	4	50×10^6	-[a]	77.3
	5	50×10^6	-[a]	85.4
0.5	0	330×10^3	330×10^3	12.87
	1	370×10^3	377×10^3	55.9
	2	380×10^3	383×10^3	63.1
	3	430×10^3	440×10^3	74.9
	4	445×10^3	450×10^3	82.3
	5	445×10^3	448×10^3	92.8

[a]: Test was not performed.

diverse amount of titanium isopropoxide were used. Hydrolysis was carried out at 60-65 °C by controlled drop-wise of titanium isopropoxide in the presence of specified graphene oxide, under ultrasonic irradiation for 1 h. The treated samples were dried at 60 °C for 30 min followed by curing at 110 °C for 4 min. The exact formation and tests results for each sample examined in this study are summarized in Table 1.

Finally, the graphene oxide/TiO_2 nanocomposite was chemically converted by reduction using sodium hydrosulfite to graphene/TiO_2 nanocomposite. Briefly, The graphene oxide/TiO_2-coated fabrics were immersed in 100 m*l* aqueous solution of sodium hydrosulfite (1 wt.%). The mixture was kept at 90 °C for 30 min under constant stirring. The resulting fabric was washed with deionized water. At the end, the fabrics were dried at 60 °C for 30 min.

Test Methods

Discoloration of Methylene Blue

The photocatalytic activities of treated fabrics were evaluated by decomposition of the methylene blue under sunlight irradiation in water. The concentration of dye in the solution was calculated by Varian Cary 300 UV-Vis spectrophotometer using calibration curve. A computer program determines absorbance of dye solution at maximum wavelength of methylene blue - 663 nm. The first step was the preparation of dye solution by distilled water (10 mg/*l*). Then, the wool samples (5×5 cm^2) were added into 100 m*l* of the dye solution. Firstly, the solution mixture was stirred for 15 min without irradiation in order to get equilibrium of dye adsorption. Then the solution was irradiated with sunlight (Tehran, Iran) for 3 consecutive days. The dye solution was continuously stirred with rate of 200 rpm and the real dye solution pH. After irradiation, the decolorization and photocatalytic degradation efficiency have been calculated as:

$$\text{Efficiency (\%)} = (C_0 - C_e)/C_0 \times 100 \quad (1)$$

where C_0 and C_e correspond to the initial and final concentration of dye before and after sunlight-irradiation. In this equation E% show the dye photocatalyst degradation percent [29].

Durability to Washing

To evaluate the durability of coatings on wool, the electrical surface resistivity of the samples was measured after laundering. The treated samples with 0.5 % of the graphene oxide were washed at 60 °C for 20 min using a solution containing 1 g/*l* nonionic detergent (Ultravon GPN, Ciba Co., Germany). Finally, samples were rinsed with distilled water and dried at room temperature.

Microbiological Test

The antimicrobial activity of the samples was evaluated against *Escherichia coli* (*E. coli*, ATCC 25922, Gram-negative bacterium) and *Staphylococcus aureus* (*S. aureus*, ATCC 25923, Gram-positive bacterium) using AATCC 100-2004 test method. This method is specially designed for specimens treated with non-releasing antibacterial agents under dynamic contact conditions. Antimicrobial activity was expressed in terms of the percentage reduction of the microorganisms and calculated as:

$$\text{Percentage reduction of microorganisms (R)\%} = (A - B)/A \times 100 \quad (2)$$

where, A and B are the number of microorganisms colonies on untreated and treated fabrics; respectively.

There was 3.4×10^5 colony forming units (cfu) of bacteria in the primary inoculum. Saline solution 8.5 g/*l* sodium chloride to 1000 m*l* distilled water was used as the neutralizing solution. Serial dilution of 10-10,000 was made for incubation on agar plate. Tryptic soy agar (Merck, Germany) was applied as the agar.

Cytotoxicity Test

The cell toxicity of the treated fabrics carried out by utilizing MTT assay. Normal primary human skin fibroblast isolated from the dermis of neonatal foreskins was used. Cell culture was performed at a 37 °C and 5 % CO_2 condition using Dulbecco's modified Eagles medium (DMEM, Biochrom, Germany) supplemented with 10 % fetal calf serum (FCS, Biochrom, Germany). Cells of the third passage were used and seeded in a 96-well microplate at a density of 20000 cells per well and incubated for 48 h. Then, the wool samples (1 inch×1 inch) were soaked in 2 m*l* culture medium for 24 h. The cultured medium with leaching substance was added to the cells and incubated for 24 h. The test samples were removed from the cell cultures, and the cells were reincubated in fresh medium. After incubation for 24 h, the cell viability was determined by means of the MTT assay [30,31]. At least three data were averaged.

Results and Discussion

FE-SEM Images, EDS Spectra and X-ray Mapping Images

In order to study the morphology of treated and untreated wool samples, a field emission scanning electron microscopy (FE-SEM) was used. The FE-SEM images of blank wool (A), wool treated with graphene oxide (B and C), wool treated with TiO_2 nanoparticles (D-F), and wool treated with graphene/TiO_2 nanocomposite (G-I) are illustrated in Figure 1. The wool treated fabric with graphene oxide surface displayed some corrugations while the raw wool fabric surface had been covered with scales, overlapping each other. It clearly reveals the presence of graphene oxide sheets on the wool fabrics. Also, it is thoroughly possible to recognize the titanium dioxide nanoparticles on the surface of wool fabric treated with nano-TiO_2 *via* comparing Figure 1(A) with Figure 1(D-F). Through the FE-SEM images of graphene/TiO_2-coated wool fabric the presence of titanium dioxide nanoparticles on the graphene sheets was confirmed (Figure 1(G-I)). It reveals that graphene is decorated with

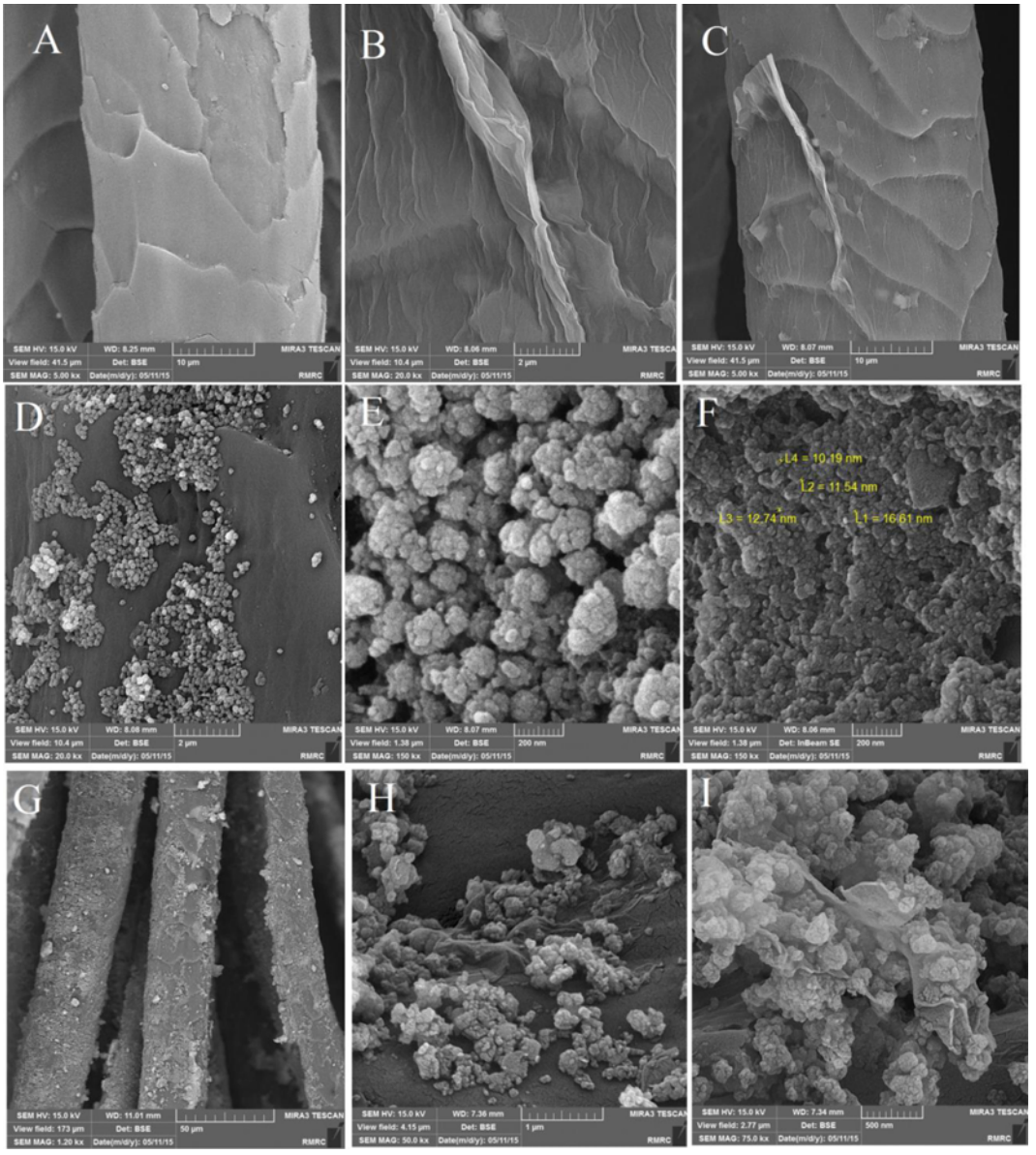

Figure 1. FE-SEM images of various wool samples: (A) raw, (B and C) treated with graphene oxide (0.5 %), (D-F) treated with TiO_2 (5 m*l* titanium isopropoxide), (G-I) treated with TiO_2/graphene nanocomposite (5 m*l* titanium isopropoxide/0.5 % graphene oxide).

TiO_2 nanoparticles densely. The average sizes of the TiO_2 nanoparticles are in the range of 10-17 nm.

Figure 2 shows the EDS spectrum of treated wool fabric with graphene/TiO_2 nanocomposite. The results show the presence of C, O, S, and Ti in the sample, which further demonstrated the successful formation of graphene/TiO_2 nanocomposite on the wool surface. Further, the distribution of C, O, S, and Ti elements in treated wool sample with graphene/TiO_2 nanocomposite was studied by the elemental mapping. As shown in Figure 3, the distribution of titanium atoms for coated wool with graphene/TiO_2 nanocomposite is uniform.

XRD Pattern

Crystalline status of the graphene/TiO_2 nanocomposite over wool fabrics was studied by XRD. The XRD pattern of coated wool fabric using graphene/TiO_2 nanocomposite is shown in Figure 4. Two major peaks can be observed around 2θ=16.4° and 22.2° related to diffraction peaks of wool. The spectrum reveals the clear peaks of titanium dioxide including anatase and rutile structures. Anatase phase main peaks are seen around 2θ=25.3°, 38.2° and 78.3°, and in 2θ=44.4° and 64.9° the peaks of rutile structure of TiO_2 exist. Also, no diffraction peaks of graphene can be seen, indicating the absence of layer-stacking regularity of graphene

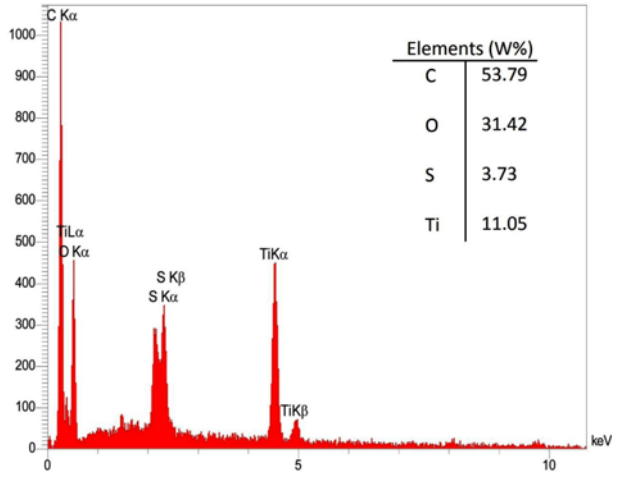

Figure 2. EDS spectrum of treated wool fabric with graphene/TiO_2 nanocomposite (0.5 % graphene oxide/5 m*l* titanium isopropoxide).

on the wool fabric. In addition, based on equation (3), the crystal size was calculated and for graphene/TiO_2 nanocomposite treated wool was 127 Å.

$$\text{Crystal size (Å)} = (K \times \lambda \times 180)/(\text{FWHM} \times \pi \times \cos\theta) \quad (3)$$

where, K=0.9 is the shape factor, λ=1.54 is the wavelength of X-ray of Cu radiation, FWHM is full width at half maximum of the peak and θ is the diffraction angle [32].

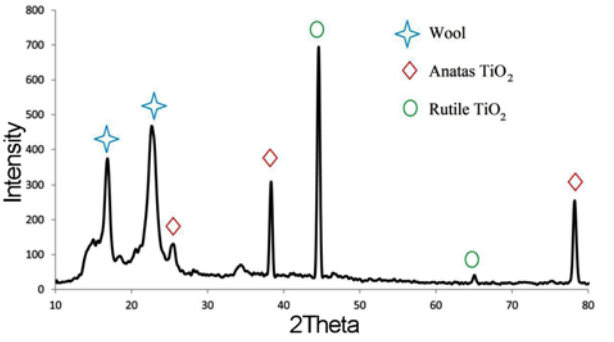

Figure 4. XRD pattern of treated wool fabric with graphene/TiO_2 nanocomposite (0.5 % graphene oxide/5 m*l* titanium isopropoxide).

Electrical and Electrochemical Properties

The blank wool, TiO_2 treated wool, graphene oxide treated wool, and graphene oxide/TiO_2 treated wool fabrics were not electroconductive (electrical resistivity in the range of 1×10^9-2×10^9 ohm/square). After reduction of graphene oxide (or graphene oxide/TiO_2) coated wool samples by sodium hydrosulfite, the electrical resistivity of the samples was reduced, in other words, its electrical conductivity increased, which indicated the effective reduction of oxygen functional groups from the graphene oxide. The electrical resistivity

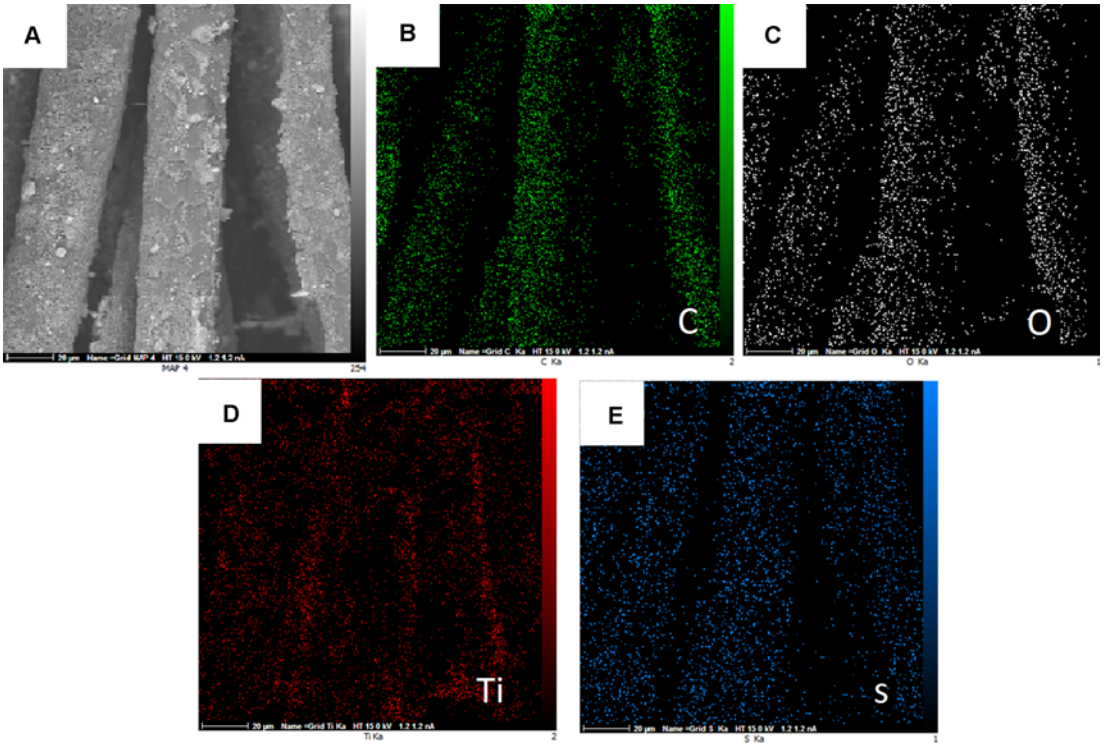

Figure 3. X-ray mapping images of treated wool fabric with graphene/TiO_2 nanocomposite (0.5 % graphene oxide/5 m*l* titanium isopropoxide). (A) microscopic image, (B) carbon atoms, (C) oxygen atoms, (D) titanium atoms, and (E) sulfur atoms.

variation of treated wool samples are presented in Table 1. Based on the obtained results, the electrical resistivity of treated wool samples decreased from 495×10^6 ohm/square to 330×10^3 ohm/square by increasing the amount of graphene oxide from 0.02 w/v % to 0.5 w/v % in the impregnating bath. The increase in graphene oxide concentration had a tangible effect on electrical conductivity of coated wool fabrics, and the electrical resistivity of treated samples diminished progressively due to the higher graphene content that produces a better contact between the graphene sheets. Also, by increasing the amount of titanium isopropoxide, the electrical conductivity decreases, which is due to the aggregation of titania nanoparticles on graphene sheets. The condensed deposition of nano-TiO_2 results in charge transfer to the graphene and a reduction of graphene mobility by charged impurity scattering [33]. Moreover, as shown in Table 1, laundering did not cause any remarkable changes in electrical resistivity of the treated samples with 0.5 % graphene oxide.

The reduction of the oxygen-containing groups in graphene oxide by sodium hydrosulfite was studied by X-ray photoelectron spectroscopy (XPS). The survey spectrum of the graphene/TiO_2 nanocomposite clearly indicates the existence of C, O and Ti in the sample (Figure 5(A)). In order to get better insight into the chemical composition of the samples, a high resolution scan was accomplished in C and Ti regions. In the case of graphene oxide (Figure 5(D)), deconvolution results in four peaks at 284.8 (C-C), 286.2 (C-OH), 287.7 (C=O bonds) and 289 eV (O=C-OH). While in the spectrum of graphene/TiO_2 nanocomposite (Figure 5(C)), in comparison to graphene oxide, most of the C-O and C=O peaks are greatly weakened. It obviously exhibits a decreased intensity for peaks corresponding to oxygen functional groups, indicating graphene oxide was effectively reduced. In addition, the band located at 283.8 eV in the nanocomposite can be assigned to the Ti-C bond.

Formation of the Ti-C bond also can be examined and confirmed by analysis of the Ti 2p core level of the XPS spectrum (Figure 5 (B)). The peaks located at 459 and 464.5 eV were assigned to the Ti 2p3/2 and Ti 2p1/2 spin-orbital splitting photoelectrons in the Ti^{4+} chemical state, respectively. The peak deconvolution of the nanocomposite indicated two other weak peaks which were attributed to formation of a Ti-C bond in the sample. Consequently, the results established the close interfacial contacts between titanium dioxide and graphene, which could be beneficial for photocatalytic performance of the nanocomposite due to the effective charge separation and transfer.

To further illustrate the reduction of graphene oxide, cyclic voltammetry was performed on samples. Figure 6 shows cyclic voltammograms (CVs) obtained for the wool coated graphene oxide/titanium dioxide nanocomposite and the wool coated graphene/titanium dioxide nanocomposite as working electrodes in supporting electrolyte. The wool coated graphene oxide/TiO_2 nanocomposite has only baseline and poor electrochemical response. However, for the wool coated graphene/titanium dioxide nanocomposite the peak current is more noticeable indicating greater electroactive surface area. These results indicated the considerable reduction

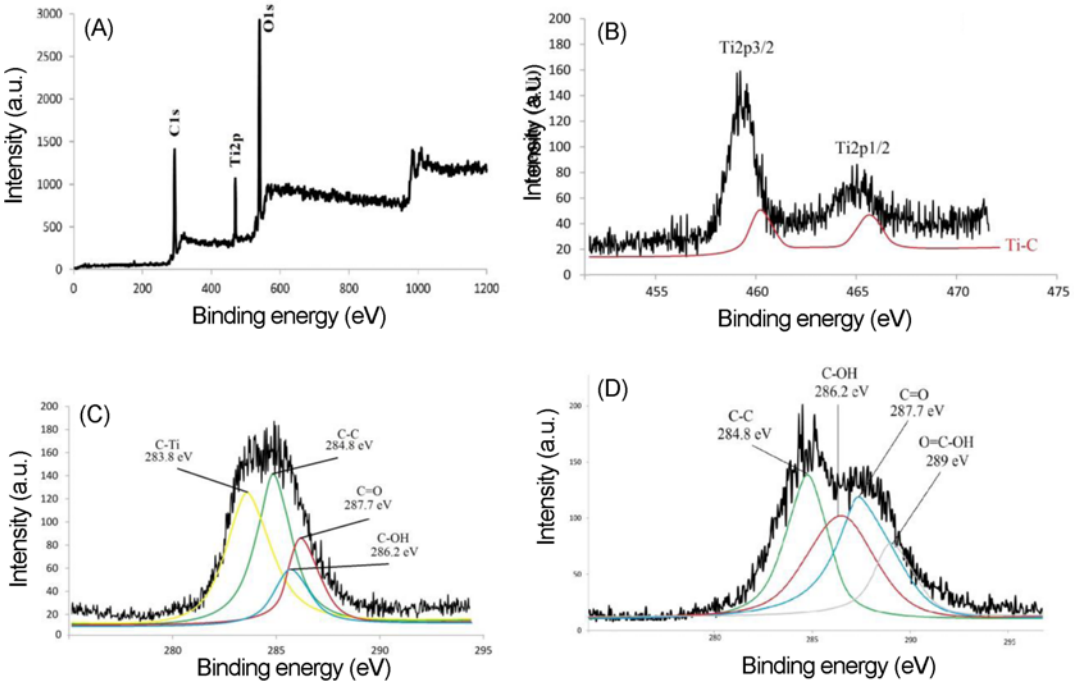

Figure 5. XPS spectra of graphene/TiO_2 nanocomposite: (A) survey, (B) Ti 2p core level, (C) C 1s core level, and (D) C 1s core level XPS spectrum of graphene oxide.

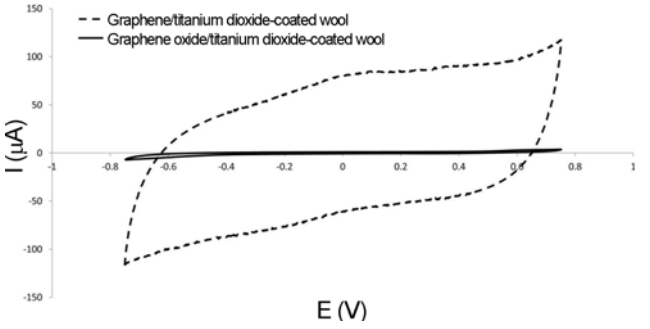

Figure 6. CVs of the graphene oxide/TiO_2-coated wool fabric and graphene/TiO_2-coated wool fabric in 0.1 M phosphate buffered saline (pH 7.0) at scan rate 50 mVs^{-1}.

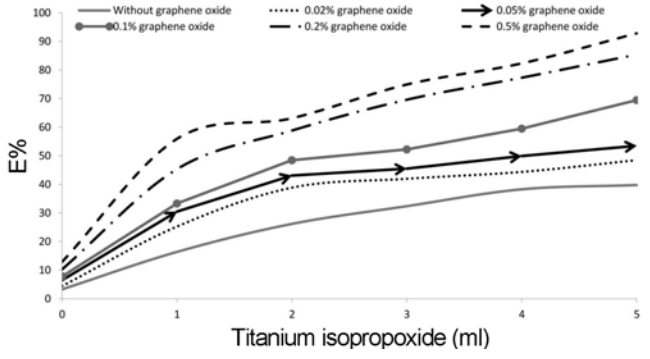

Figure 7. Comparative diagram of photocatalytic performance results of the wool samples.

of graphene oxide and the successful preparation of the graphene/titanium dioxide nanocomposite on wool fabric.

Photocatalytic Performance

Photocatalytic performance of the treated wool fabrics were estimated by the rate of decomposition of the dye under sunlight irradiation. The photo-activity efficiencies of the samples are shown in Table 1 and Figure 7. It can be observed that the methylene blue concentration change was negligible during irradiations in contact with blank wool. Loading of graphene in wool fabric led to decrease in methylene blue concentration due to adsorption of methylene blue by graphene sheets [34]. Therefore, the blank wool and the graphene-coated wool fabrics show no photocatalytic activity under sunlight irradiation. The treated wool samples with titanium isopropoxide showed higher dye decomposition ability. Also, more titanium isopropoxide led to the better photocatalytic activity (E%) possibly due to more TiO_2 nanoparticles absorption by the fabric. When the photocatalyst is illuminated by a light with energy higher than its bandgap energy, electron-hole pairs diffuse out to the surface of the photocatalyst. The created negative electrons and oxygen combine into O_2^-, and the positive electric holes and water generate hydroxyl radicals. This highly active oxygen species can oxidize organic pollutants. Thus, nano titanium dioxide can decompose common organic matters, dye molecules, bacterial cell membrane, etc. [35].

As shown in Figure 7, the nanocomposite-coated samples confirmed more photocatalytic degradation of methylene

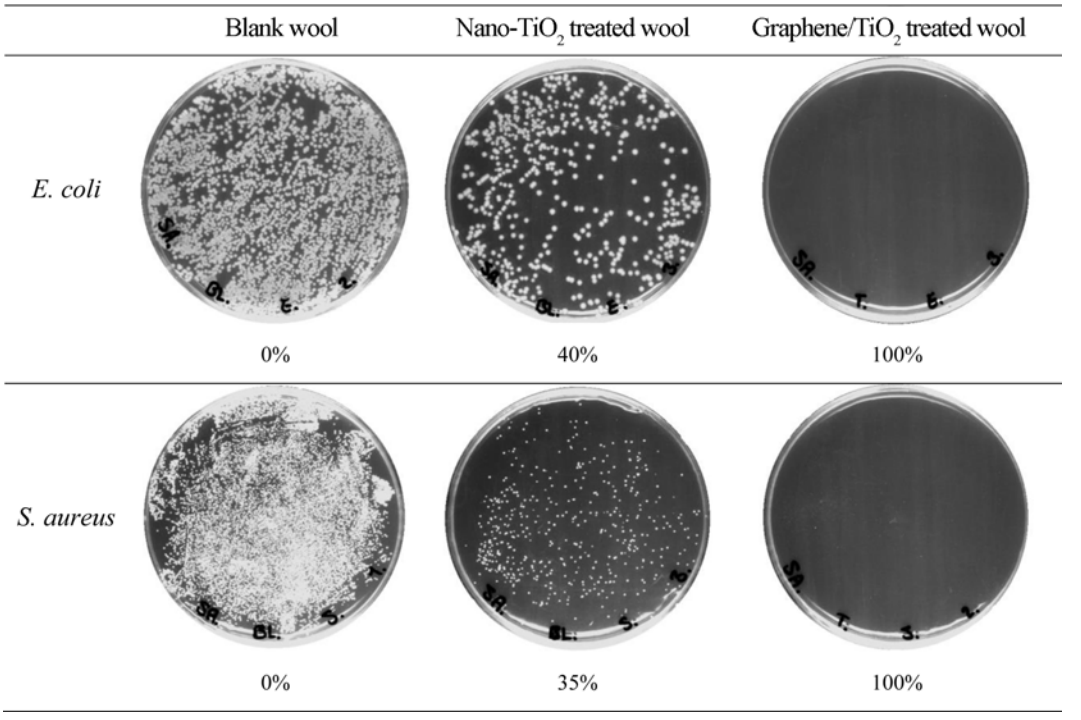

Figure 8. The antibacterial efficiency of the wool samples.

blue in comparison with nano TiO_2-coated wool fabrics. It is because graphene in graphene/TiO_2 nanocomposite, promotes the separation of electron-hole pairs and extends the life of electrons. Also, the adsorption of dye molecules is helpful for the increase of photocatalytic activity. Furthermore, the extended light absorption ability of graphene/TiO_2 nanocomposite improves the photocatalystic performance [24,25].

Antibacterial Property and Cell Viability

The percentage of the bacteria reduction by nano-TiO_2 treated wool, graphene/TiO_2 treated wool, and blank wool is reported in Figure 8. As expected, the blank wool fabrics provide a suitable environment for growth of microorganisms. The graphene/TiO_2 treated sample indicated higher bactericidal activity than nano-TiO_2 treated sample due to high surface area of graphene. Therefore, adding graphene to titanium dioxide nanoparticles can also facilitate effective bacterial decomposition by increasing the contact between the catalyst nanoparticles and the bacteria [26].

Cytotoxicity test of the graphene/TiO_2 treated wool fabric and blank wool fabric was examined by MTT assay. The cell viability and morphology of human fibroblast cells are presented in Figure 9. Based on the obtained results, the treated fabrics with graphene/titanium dioxide nanocomposite have low cytotoxicity, similarly to the blank samples. Moreover, the morphology of fibroblast cells in presence of the treated wool fabric is normal, which is similar to the morphology of the blank wool sample. Therefore, no significant cytotoxicity effect was established by the nanocomposite treated fabrics on human skin.

UV Blocking

The UV transmittance spectra of blank wool fabric and treated wool fabric with graphene/TiO_2 nanocomposite (in the range of 280-400 nm) were illustrated in Figure 10. The upper line is the UV transmittance spectrum of the raw wool sample demonstrating that high percentage of the UV light can penetrate into the fabric. The graphene/TiO_2 nanocomposite treated wool fabric had much lower UV transmittance compared to the raw wool fabric. Consequently, the treated wool fabrics with graphene/TiO_2 nanocomposite have good

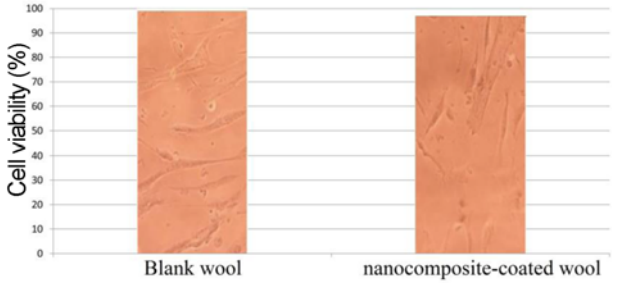

Figure 9. Cell viability properties of the untreated and graphene/TiO_2 treated fabrics.

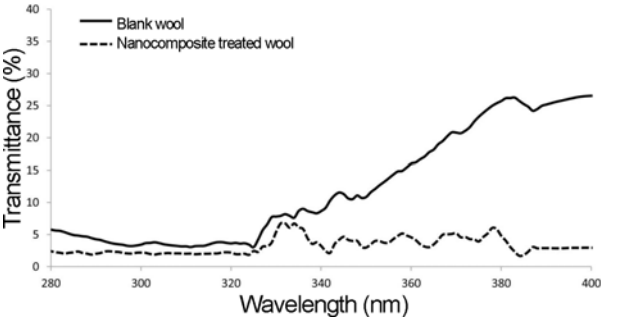

Figure 10. UV transmittance spectra of blank wool fabric and treated wool fabric with graphene/TiO_2 nanocomposite.

UV blocking property due to the synergetic UV absorption of titanium dioxide and graphene [36].

Conclusion

For the first time, graphene/titanium dioxide nanocomposites were successfully synthesized on the wool fabric as a novel finishing technique. Incorporating graphene/TiO_2 nanocomposite on the wool fabrics formed functional characteristics including self-cleaning, antibacterial, electrical conductivity, electroactivity with low cytotoxicity and higher UV blocking. Through FE-SEM and X-ray mapping images, XPS spectra, XRD and EDS patterns the presence of graphene/TiO_2 nanocomposite on the surface of the treated wool fabrics was confirmed. All properties of the treated wool with graphene/titanium dioxide nanocomposite were superior compared to the treated wool with nano titanium dioxide alone. It is expected graphene/TiO_2 nanocomposite might be used to produce high performance fabrics and smart textiles.

Acknowledgments

I would like to express my appreciation to Yazd Branch, Islamic Azad University for its support of research project under the title of *in-situ* synthesis of graphene/titanium dioxide nanocomposite on wool fabric and its properties.

References

1. N. A. G. Johnson and I. Russell, “Advances in Wool Technology”, 1rd ed., pp.176-177, Woodhead Publishing Limited, Cambridge, 2009.
2. M. Montazer, E. Pakdel, and M. B. Moghadam, *Fiber. Polym.*, **11**, 967 (2010).
3. E. Pakdel, W. A. Daoud, and X. Wang, *Appl. Surf. Sci.*, **275**, 397 (2013).
4. M. Li, T. Deng, S. Liu, F. Zhang, and G. Zhang, *Appl. Surf. Sci.*, **297**, 147 (2014).
5. S. Zohoori and L. Karimi, *Fiber. Polym.*, **14**, 996 (2013).
6. F. Lessan, M. Montazer, and M. B. Moghadam, *Thermochim.*

Acta, **520**, 48 (2011).
7. G. Y. Bae, Y. G. Jeong, and B. G. Min, *Fiber. Polym.*, **11**, 976 (2010).
8. M. P. Gashti, F. Alimohammadi, and A. Shamei, *Surf. Coat. Technol.*, **206**, 3208 (2012).
9. M. P. Gashti and A. Almasian, *Compos. Pt. B-Eng.*, **52**, 340 (2013).
10. M. P. Gashti, A. Almasian, and M. P. Gashti, *Sens. Actuator A-Phys.,* **187**, 1 (2012).
11. F. Alimohammadi, M. P. Gashti, and A. Shamei, *J. Coat. Technol. Res.*, **10**, 123 (2013).
12. Y. Liu, X. Wang, K. Qi, and J. H. Xin, *J. Mater. Chem.*, **18**, 3454 (2008).
13. F. Zhang, X. Wu, Y. Chen, and H. Lin, *Fiber. Polym.*, **10**, 496 (2009).
14. L. Budama, B. A. Çakır, Ö. Topel, and N. Hoda, *Chem. Eng. J.*, **228**, 489 (2013).
15. M. Montazer and E. Pakdel, *J. Photochem. Photobiol. C*, **12**, 293 (2011).
16. C. N. R. Rao, A. K. Sood, K. S. Subrahmanyam, and A. Govindaraj, *Angew Chem. Int. Edit,* **48**, 7752 (2009).
17. C. Soldano, A. Mahmood, and E. Dujardin, *Carbon,* **48**, 2127 (2010).
18. J. Molina, J. Fernández, A. I. del Río, J. Bonastre, and F. Cases, *Appl. Surf. Sci.,* **279**, 46 (2013).
19. J. Molina, J. Fernández, M. Fernandes, A. P. Souto, M. F. Esteves, J. Bonastre, and F. Cases, *Synth. Met.*, **202**, 110 (2015).
20. I. A. Sahito, K. C. Sun, A. A. Arbab, M. B. Qadir, and S. H. Jeong, *Carbohydr. Polym.,* **130**, 299 (2015).
21. B. Fugetsu, E. Sano, H. Yu, K. Mori, and T. Tanaka, *Carbon,* **48**, 3340 (2010).
22. L. Qu, M. Tian, X. Hu, Y. Wang, S. Zhu, X. Guo, G. Han, X. Zhang, K. Sun, and X. Tang, *Carbon,* **80**, 565 (2014).
23. J. Zhao, B. Deng, M. Lv, J. Li, Y. Zhang, H. Jiang, C. Peng, J. Li, J. Shi, Q. Huang, and C. Fan, *Adv. Healthcare Mater.,* **2**, 1259 (2013).
24. L. M. Pastrana-Martínez, S. Morales-Torres, S. K. Papageorgiou, F. K. Katsaros, G. E. Romanos, J. L. Figueiredo, J. L. Faria, P. Falaras, and A. M. T. Silva, *Appl. Catal. B-Environ.*, **142**, 101 (2013).
25. S. Liu, H. Sun, S. Liu, and S. Wang, *Chem. Eng. J.*, **214**, 298 (2013).
26. L. Karimi, M. E. Yazdanshenas, R. Khajavi, A. Rashidi, and M. Mirjalili, *Cellulose*, **21**, 3813 (2014).
27. L. Karimi, M. E. Yazdanshenas, R. Khajavi, A. Rashidi, and M. Mirjalili, *Appl. Surf. Sci.,* **332**, 665 (2015).
28. J. Molina, F. Fernandes, J. Fernández, M. Pastor, A. Correia, A. P. Souto, J. O. Carneiro, V. Teixeira, and F. Cases, *Mater. Sci. Eng. B*, **199**, 62 (2015).
29. L. Karimi, S. Zohoori, and M. E. Yazdanshenas, *J. Saudi Chem. Soc.,* **18**, 581 (2014).
30. A. Behzadnia, M. Montazer, and M. M. Rad, *Ultrason. Sonochem.,* **27**, 10 (2015).
31. A. Behzadnia, M. Montazer, and M. M. Rad, *J. Photochem. Photobiol. B,* **149***,* 103 (2015).
32. M. Montazer and E. Pakdel, *Photochem. Photobiol.*, **86**, 255 (2010).
33. K. M. McCreary, K. Pi, and R. K. Kawakami, *Appl. Phys. Lett.*, **98**, 192101 (2011).
34. J. Liu, H. Bai, Y. Wang, Z. Liu, X. Zhang, and D. D. Sun, *Adv. Funct. Mater.,* **20**, 4175 (2010).
35. S. Zohoori, L. Karimi, and S. Ayaziyazdi, *J. Ind. Eng. Chem.,* **20**, 2934 (2014).
36. Y.-K. Kim and D.-H. Min, *Nanoscale,* **5**, 3638 (2013).